Effects of lithology and acid mine drainage on Cd concentration and isotope distribution in a large riverine system, Guangxi Province, South China

Zhengbing Zhou [a], Hanjie Wen [b,c,*], Chuanwei Zhu [d], Bo Bao [e], Chongguang Luo [d], Yuxu Zhang [d]

[a] State Key Laboratory of Nuclear Resources and Environment, East China University of Technology, Nanchang 330013, PR China
[b] School of Earth Sciences and Resources, Chang'An University, Xi'an 710054, PR China
[c] University of Chinese Academy of Sciences, Beijing 100049, PR China
[d] State Key Laboratory of Ore Deposit Geochemistry, Institute of Geochemistry, Chinese Academy of Sciences, Guiyang 550081, PR China
[e] Wuhan Center, China Geological Survey (Central South China Innovation Center for Geosciences), Wuhan 430205, PR China

ARTICLE INFO

ABSTRACT

Cadmium is highly toxic to plants, animals, and humans. When assessing its risk, it is critical to distinguish anthropogenic activities from natural weathering processes. Specific Cd isotopes have been used to track the source and fate of Cd in the environment. However, Cd isotopic signatures in soils and sediments and its fractionation in large river systems, especially in high-population areas and within complex Cd source regions, remain poorly understood. Using chemical and isotope analyses, this study identifies Cd sources in the Xijiang riverine system, China, as being the result of natural weathering and acid mine drainage. Cadmium isotopic fractionation between stream sediment and topsoil was uniform, with $\Delta^{114/110}Cd_{stream\ sediment–topsoil}$ values averaging 0.50‰ ± 0.04‰ through natural weathering processes and fractionation being controlled mainly by the Cd isotopic composition of acid mine drainage. During the natural weathering of carbonate sediments, Ca^{2+} and HCO_3^- in soils tend to drain into the Xun River with leachate, resulting in a weakly alkaline water column with increasing Cd contents in stream sediments. In mining regions, H^+, Cd^{2+}, Zn^{2+}, and other metal ions are prone to release from sphalerite into solution under supergene conditions, ultimately resulting in high Cd contents in sediments of the Meng River. This study highlights the use of $\Delta^{114/110}Cd_{stream\ sediment–topsoil}$ values as a tool for distinguishing the effects of anthropogenic activities from those of natural weathering processes in river systems at risk of Cd pollution.

1. Introduction

Cadmium is highly toxic, and uptake via ingestion, skin contact, and inhalation results in the accumulation of Cd in human and animal tissues such as the liver and kidneys (Satarug et al., 2004; Aoshima, 2016), causing various health issues. Cadmium pollution is thus a significant environmental issue globally, and Cd is classified as a critical metal pollutant in many countries including China and the USA (MEPPRC and MLRPRC, 2014; Scott et al., 2019; Wang et al., 2020). Anthropogenic activities including mining, smelting, Ni − Cd battery manufacture and disposal, mineral phosphate fertiliser and manure use, and wastewater irrigation discharge large amounts of Cd into the terrestrial environment. The resultant atmospheric deposition is also a source of contamination. Soils and sediments are important Cd sources because they discharge Cd into the water column through chemical and biological

processes, and uptake by plants allows Cd to enter food chains (Wei et al., 2019). River systems may thus promote Cd migration from local to regional distribution. Previous studies have shown that Cd contents in soils and stream sediments are related to those in parent rocks affected by natural weathering (Zhao et al., 2015; Wen et al., 2020) or anthropogenic activities (Cloquet et al., 2006; Wen et al., 2015; Zhang et al., 2016; Zhong et al., 2020, 2021). In general, Cd contents in the soils of karst regions (mean 0.6 $\mu g.g^{-1}$) are higher than those of non-karst regions (mean 0.15 $\mu g.g^{-1}$) (Li et al., 2021; Yaciuk et al., 2022), and both natural weathering and anthropogenic activity potentially lead to Cd accumulation in soils. It is thus critical to identify Cd sources in Cd-polluted areas to improve our understanding of Cd behaviour and enrichment mechanisms in the environment, which may help to select an appropriate remediation technique and lead to reductions in Cd exposure (Wen et al., 2015; Ratie et al., 2022). The development of

improved analytical procedures and multi-collector–inductively coupled plasma–mass spectrometry (MC–ICP–MS) allow the determination of minor fractionation of stable Cd isotopes in geological samples and its application in improving our understanding of biogeochemical processes, the paleo-environment, and hydrothermal systems (Gao et al., 2013; Wei et al., 2016; Yan et al., 2020; Zhang et al., 2018; Zhu et al., 2017). Cadmium isotopes have been used to track the source and fate of Cd in the environment, and Cd from different sources often has distinct isotopic characteristics (Cloquet et al., 2006; Gao et al., 2013; Zhang et al., 2016; Martinkova et al., 2016; Yin et al., 2021; Zhong et al., 2021). Anthropogenic activities could produce large Cd isotopic fractionation and thus may be distinguishable from terrestrial samples (Cloquet et al., 2006; Wen et al., 2015; Chrastny et al., 2015; Martinkova et al., 2016; Ratie et al., 2022). Cloquet et al. (2006) reported that the $\delta^{114/110}$Cd values of slag and dust from a smelter in northern France were in 1.0‰ difference. Chrastny et al. (2015) reported the Cd isotopic fractionation ($\Delta^{114/110}$Cd) between granulated waste and final refinement waste near the Olkusz Pb—Zn smelter were up to 0.6‰. Martinkova et al. (2016) detected Cd isotope of industrial materials and shown significant Cd isotopic fractionation in various technological processes. Besides, recent studies have confirmed that natural weathering can cause significant Cd isotopic fractionation during sulphide oxidation in supergene environments, with $\Delta^{114/110}$Cd$_{fluid–solid}$ values of up to ~0.5‰ (Zhang et al., 2016; Zhu et al., 2018), so it is critical to distinguish the influence of anthropogenic activities from natural weathering when using Cd

isotopes to track Cd sources. However, the Cd isotopic signatures of soils and sediments in large river systems, especially in high-population areas, remain poorly constrained.

In this study, we investigated the Cd contents and isotopic compositions and major- and -trace element compositions of Xijiang River stream sediments and topsoils in Guangxi Province, South China (Fig. 1). The Xijiang River is the largest river in the Pearl River watershed. Guangxi Province contains giant Zn–Sn–Sb polymetallic deposits such as the Dachang, Jianzhupo, Beishan, and Siding deposits, which have Zn reserves of up to 13 megatonnes (Cai, 2015; Yang et al., 2017; Zhang et al., 2020). The drainage basin of the Xijiang River is mainly composed of Devonian limestone, glutenite and Yanshanian granite (Fig. 1c; Wang et al., 2012; Yang et al., 2017; Pang, 2020). Widespread carbonate sediments are distributed at the upper reaches, and the lower alluvial plain is mainly composed the Quaternary sediments and alluvial deposits (Fig. 1c; Pang, 2020). Mining and refining activities cause discharge of Cd from deposits to rivers and soils. Recent studies have shown that heavy-metal contents in most river sediments of the Guangxi region exceed accepted safety limits, indicating high ecological and environmental health risks (Song et al., 2018). Through the analysis of stream sediments and riverine soils, we investigated variations in Cd contents and isotopic compositions to identify the sources of Cd (anthropogenic or natural), with the aim of improving our understanding of Cd dissemination in river systems and the evaluation of heavy-metal contamination of the environment.
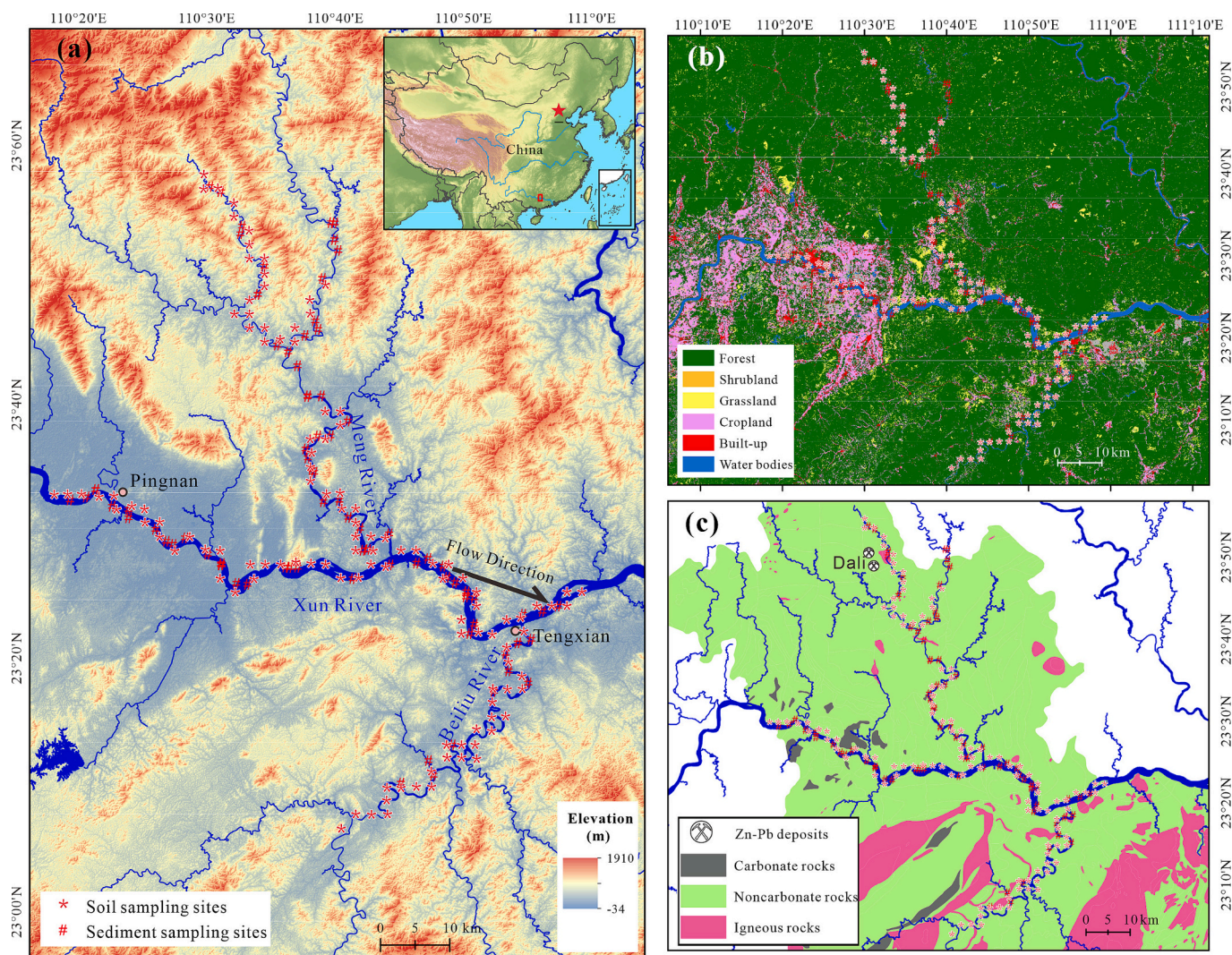

Fig. 1. Sampling sites (a), land uses (b) and, lithology (c) map in the Xijiang River.

2. Materials and methods

2.1. Sample collection and preparation

The Xijiang River is the largest river in Guangxi Province and flows 1248 km in a generally southeasterly direction to the South China Sea. Its total watershed area is 202,100 km^2, comprising >85% of the total land area of Guangxi Province. Owing to the increasing development of mining and other industries over recent decades, many sections of the water system have incurred heavy-metal contamination of sediments and riverbank soils, thus posing an ecological risk to local humans and animals (Zhao et al., 2020).

Samples were collected from Wuzhou City (Fig. 1), where the Xijiang River divides into three tributaries, the Xun, Meng, and Beiliu rivers. A total of 48 topsoil and 35 stream sediment samples were collected along the Xun River, and 41 soil and 35 stream sediment samples were collected along the Meng River, at intervals of ~2 km (Appendix A). The water flow in the Beiliu River is the lowest of the three tributaries, and 29 soil and 10 stream sediment samples were collected (Appendix A). Soil sampling sites were selected on the basis of a regular grid suggested by the China Geology Survey (CGS, 2005), with a density of 1 sample km^{-2}. Sampling locations were determined using a global positioning system instrument (Garmin, USA). Sample representative was assured by mixing four subsamples of ~50 g, collected at 0–20 cm depth within 1 km^2. Potentially high anthropogenic activity areas (e.g., roadsides and factories) were avoided. A sediment sampler was used for the collection of surface sediments from 0 to 20 cm depth, with a wet weight of ~3 kg.

After collection, stream sediment samples and topsoil samples were dried to constant weight at 70 °C over 24 h. The dried samples were then crushed to <74 μm particle size using an agate mortar. Measurements of topsoil pH were carried out in the laboratory by a portable pH meter (HQ40D, Hach, USA). 4 g samples were weighted into a Teflon beaker with reagents of 10 ml distilled water, and then stirred for 1 min on a magnetic stirrer. After standing for 30 min, pH value was obtained by the pH meter.

2.2. Chemical analyses of topsoil and stream sediment

Contents of major-element oxides (SiO$_2$, Al$_2$O$_3$, Fe$_2$O$_3$, MgO, CaO, Na$_2$O and K$_2$O) were determined by wavelength-dispersive X-ray fluorescence (XRF; ARL Perform'X 4200) at the State Key Laboratory of Ore Deposit Geochemistry (SKLODG), Institute of Geochemistry, Chinese Academy of Sciences. XRF data were calibrated using a "standard-less" method. Three US National Institute of Standards and Technology (NIST) reference standards were used in Uniquant data processing (Dai et al., 2015). The relative standard deviations (RSDs) of the results were <10%.

Trace-element contents were determined by ICP–MS (PlasmaQuant MS Elite) at the SKLODG. Samples of 50 mg were weighed into digestion tubes for microwave digestion (ultra CLAVE, Milestone) with reagents of 2 ml distilled HF and 5 ml distilled HNO$_3$. Digestion temperature was 180 °C for 2 h. After digestion, the samples were transferred to Teflon beakers for evaporation to dryness on a hotplate at 100 °C. Samples were then treated with 3 ml concentrated HNO$_3$ at 110 °C for ~24 h before drying again at 100 °C. Finally, 10 ml 2% HNO$_3$ (v/v) was added and the solution transferred to a 15 ml polypropylene centrifuge tube. After centrifugation, the supernate was used for analysis. GSP-2 and BHOV-2 were prepared to monitor the digestion processes and to control the quality of the obtained data. The elemental concentration values for these reference materials are shown in Appendix B. The RSD for trace-element analyses was <3%.

2.3. Cd isotope analysis

Cd separation and mass spectrometry analyses were undertaken at the SKLODG. Samples containing ~600 ng Cd were weighed into Teflon

beakers. ^{111}Cd—^{110}Cd double-spike solution (0.6 ml, 1 mg L^{-1}) was added to ensure Cd$_{spike}$/Cd$_{sample}$ ratios of ~1. The digestion procedure was similar to that used for trace elements, except that HCl (2 ml 2 mol L^{-1}) was added to the 5 ml polypropylene centrifuge tube. After centrifugation, the supernate was purified by anion-exchange chromatography using AG–MP–1 M resin (3 ml; Bio-Rad, pre-cleaned 100–200 mesh) with 24 ml 0.0012 mol.L^{-1} HCl Cd eluent, as described by Zhu et al. (2018). The eluate was evaporated to dryness at 100 °C, and the residue was dissolved in 3 ml 2% HNO$_3$ (v/v) for MC–ICP–MS analysis. Meanwhile, two Cd secondary reference standards (NIST SRM 3108 Cd, and JMC Cd) and two geological reference materials (NOD-A-1 and NOD-P-1, manganese nodules) were prepared to monitor the chemical separation and mass spectrometry measurements. The total Cd recovery of the chemical separation method was up to 95% in our study.

Isotopic Cd ratios measurements were performed at the SKLODG, using a *Thermo-Scientific Neptune plus* MC-ICP-MS instrument with a combination of Ni 'Standard' sampler cone + Ni 'X-type' skimmer cone. Sample solutions were introduced through a perfluoroalkoxy micro-flow nebulizer (ESI; 100 μL min^{-1}) connected to a double-Scott spray chamber. A low-resolution entrance slit was used. Analysed generally yielded a ^{114}Cd voltage of 5.6 V for a 200 ng ml^{-1} solution. Instrumental baseline and peak centering were done before operating the sample (standard) analysis sequence. Each measurement included 60 integration of 4.194 s for two blocks of 30 cycles for ^{110}Cd (L3 cup), ^{111}Cd (L2), ^{112}Cd (L1), ^{113}Cd (center cup), ^{114}Cd (H1), ^{115}In (H2), and ^{117}Sn (H4) measurement. Also, for beginnings of 10 cycles, we measured ^{105}Pd (center cup at sub-configurations; peak-jumping model) with integration time of 2.097 s. After every measurement, the nebulizer and spray chamber were washed with 2% HNO$_3$ (v/v) to reduce the Cd signal to an insignificant level (<0.1 mV) over 120 s of integration. The double-spike method was used to correct mass bias.

The δ values for Cd isotopes were determined as follow:

$$\delta^{x/110}Cd\ (‰) = ((^{x/110}Cd)_{sample}/(^{x/110}Cd)_{std} - 1) \times 1000,$$

where x = 111, 112, and 114.

Isotopic fractionation between stream sediment and topsoil was calculated as follows:

$$\Delta^{114/110}Cd_{sediment-topsoil} = \delta^{114/110}Cd_{stream\ sediment} - \delta^{114/110}Cd_{topsoil}.$$

Nancy Spex Cd solution (CRPG, France) was used as the zero-reference standard. NIST SRM 3108 (lot 130,116) and JMC (USA) Cd solution (lot 74-075219 k) were used as secondary reference standards. The measured values for NOD-A-1 ($\delta^{114/110}Cd = 0.13‰ \pm 0.05‰$; 2SD, $n = 3$), NOD-P-1 ($\delta^{114/110}Cd = 0.21‰ \pm 0.04‰$; 2SD, n = 3), NIST SRM 3108 ($\delta^{114/110}Cd = 0.11‰ \pm 0.05‰$; 2SD, $n = 6$), and JMC Cd solution ($\delta^{114/110}Cd = -1.57‰ \pm 0.07‰$; 2SD, n = 6) are consistent well with previous studies (Pallavicini et al., 2014; Zhang et al., 2016, 2018; Zhou and Wen, 2021).

2.4. Mass balance-based binary mixing model

It was assumed that a V_{mix} volume (m^3) of mixed water contains V_1 m^3 of unpolluted river water and V_2 m^3 of acid mine drainage and that the coefficient of Cd deposition from water to sediment is stable. C_1, C_2, and C_{mix} are the Cd contents of sediments from unpolluted river water, acid mine drainage, and mix water, respectively. Cd concentrations in these three types of water can be expressed as $k \times C_1$, $k \times C_2$, and $k \times C_{mix}$, with δ_1, δ_2, and δ_{mix} being their $\delta^{114/110}$Cd values, respectively, and f_1 and f_2 being the relative contributions of Cd from unpolluted river and acid mine drainage water, respectively. Consequently, the Cd mass and isotopic balance can then be expressed as follows:

$$(V_1 \times k \times C_1) + (V_2 \times k \times C_2) = V_{min} \times k \times C_{mix} \tag{1}$$

$$f_1 = \frac{(V_1 \times k \times C_1)}{(V_{mix} \times k \times C_{mix})} \tag{2}$$

$$f_2 = \frac{(V_2 \times k \times C_2)}{(V_{mix} \times k \times C_{mix})} \qquad (3)$$

$$f_1 + f_2 = 1 \qquad (4)$$

$$(f_1 \times \delta_1) + (f_2 \times \delta_2) = \delta_{mix} \qquad (5)$$

From Eqs. (2)–(5), δ_{mix} can be simplified as follows:

$$\delta_{mix} = (\delta_1 - \delta_2) \times \frac{(C_1 \times V_1)}{(C_1 \times V_1) + (C_2 \times V_2)} + \delta_2 \qquad (6)$$

3. Results

3.1. Chemical compositions of topsoil and sediment

The chemical compositions of topsoils and stream sediments are listed in Appendix A, summarised with means and standard deviations in Tables 1–4 and plotted in Figs. 2, S1, and S2. The compositions are described separately for each of the three river systems below.

3.1.1. The Xun River

Topsoil and stream sediment samples from the Xun River system have higher CaO and Na_2O contents than those of other riverbank samples in the region (Fig. S1). The Cd contents in 90% and 95% of topsoil samples from upstream and downstream exceed the background value of Cd for soils in Guangxi Province (0.27 $\mu g \cdot g^{-1}$), respectively. Cadmium contents in sediment are higher than those of topsoil. Below the confluence with the Meng River, a slight increase in sediment Cd content was observed. Other heavy metals such as Zn, Cu, Pb, As, Sb, Ni, and Cr display similar trends to those of Cd.

3.1.2. Meng River

Topsoil samples from the Meng River system have higher SiO_2 and K_2O contents than those concentrations of the Xun River but the lowest

Table 1
Summary of major element concentrations of topsoil samples in the Xijiang River (wt%).

Subjects	SiO₂	Al₂O₃	TFe₂O₃	MgO	CaO	Na₂O	K₂O
The Xun River upstream							
MIN	61.90	10.30	3.47	0.36	0.03	0.06	1.04
MAX	74.17	17.52	7.91	1.10	1.97	0.46	2.49
MEAN	67.13	13.74	5.99	0.72	0.47	0.25	1.70
SD	3.61	2.08	0.88	0.18	0.32	0.09	0.36
The Xun River downstream							
MIN	59.66	12.92	4.35	0.48	0.08	0.10	1.77
MAX	70.05	19.39	7.25	1.26	0.77	0.43	2.65
MEAN	65.27	15.28	6.00	0.84	0.39	0.25	2.24
SD	2.86	1.48	0.81	0.22	0.19	0.09	0.25
The Meng River							
MIN	61.80	8.07	2.70	0.34	0.07	0.06	1.08
MAX	77.97	17.66	8.09	0.75	0.30	0.13	2.50
MEAN	69.98	13.97	4.79	0.55	0.13	0.08	2.01
SD	3.57	2.13	0.95	0.09	0.05	0.02	0.34
Chentang tributary of the Meng River							
MIN	67.93	11.61	3.61	0.47	0.11	0.06	1.58
MAX	74.04	16.38	4.92	0.64	0.15	0.08	2.25
MEAN	71.22	13.99	4.38	0.54	0.12	0.07	1.99
SD	2.33	1.79	0.49	0.07	0.02	0.01	0.25
The Beiliu River							
MIN	57.04	8.64	2.06	0.25	0.10	0.06	1.23
MAX	81.07	21.12	7.47	0.84	0.53	0.33	2.87
MEAN	69.63	15.54	4.24	0.39	0.18	0.12	2.08
SD	5.61	3.12	1.24	0.13	0.07	0.06	0.42

Table 2
Summary of major element concentrations of stream sediments in the Xijiang River (wt%).

Subjects	SiO₂	Al₂O₃	TFe₂O₃	MgO	CaO	Na₂O	K₂O
The Xun River upstream							
MIN	2.92	2.33	0.44	0.87	0.22	0.77	
MAX	15.02	6.39	1.12	2.54	0.52	2.31	
MEAN	7.78	4.19	0.73	1.67	0.35	1.42	
SD	3.73	1.26	0.23	0.47	0.07	0.36	
The Xun River downstream							
MIN	10.07	4.82	0.93	0.88	0.33	1.58	
MAX	19.76	10.03	1.14	2.46	0.45	2.28	
MEAN	13.98	7.33	1.03	1.73	0.39	1.91	
SD	2.27	1.74	0.08	0.39	0.04	0.20	
The Meng River							
MIN	1.88	1.17	0.13	0.03	0.03	0.59	
MAX	12.90	9.39	0.62	1.33	0.10	2.72	
MEAN	7.20	4.27	0.41	0.17	0.07	1.87	
SD	2.82	1.63	0.13	0.26	0.02	0.54	
Chentang tributary of the Meng River							
MIN	1.91	1.41	0.13	0.03	0.03	0.66	
MAX	10.10	6.11	0.56	0.11	0.13	2.36	
MEAN	5.59	3.37	0.35	0.06	0.08	1.54	
SD	2.95	1.66	0.16	0.03	0.04	0.65	
The Beiliu River							
MIN	6.01	2.79	0.24	0.13	0.11	1.14	
MAX	14.05	8.76	0.47	1.80	0.23	2.45	
MEAN	10.11	4.72	0.38	0.41	0.18	2.01	
SD	2.77	1.68	0.08	0.49	0.03	0.38	

CaO contents of the Xijiang River systems. Stream sediment samples also have low CaO contents (Fig. S1). However, stream sediments in the lower reaches have high Ba contents, generally of >3000 $\mu g \cdot g^{-1}$, with a highest value of 5240 $\mu g \cdot g^{-1}$ (Fig. S1).

The Cd contents of topsoils near the Meng River are in the range of 0.08–0.68 $\mu g \cdot g^{-1}$, with those of 89% of samples being below the background value for Cd. However, the Cd contents of stream sediments vary widely, at 0.37–20.8 $\mu g \cdot g^{-1}$, with a maximum of 78 times the background value (0.267 $\mu g \cdot g^{-1}$). Consistent with Cd, the Zn contents of the sediments are high, exceeding the accepted safety limits. Overall, trends in the Zn, Cu, and Pb contents of topsoils and stream sediments from the Meng River are similar to those of Cd.

3.1.3. Beiliu River

Topsoil samples from the Beiliu River system have high SiO_2 contents, and the stream sediments have low CaO contents. The Cd contents of the topsoil samples are in the range of 0.08–1.22 $\mu g \cdot g^{-1}$, with those of only ~7% of the samples being slightly above the background value. Sediments have lower Cd contents, with a range of 0.12–0.55 $\mu g \cdot g^{-1}$. Contents of other heavy metals (Zn, Cu, Pb, As, Sb, Ni, and Cr) are at background levels.

3.2. Cd isotope compositions of topsoil and stream sediments from the Xun River and the Meng River

The Cd isotopic compositions of the topsoil and sediment samples collected from the Xun and Meng river are described in Table 5 and 6, respectively.

Topsoil samples from near the Xun River have a narrow range of $\delta^{114/110}Cd$ values (−0.41‰ to −0.12‰; mean − 0.28‰ ± 0.06‰; 1SD, $n = 17$), with those of the upper reaches being consistent with those of the lower reaches (Table 5). Stream sediment samples have higher $\delta^{114/110}Cd$ values with an overall range of −0.05‰ to 0.29‰ (mean 0.14‰ ± 0.11‰; 1SD, $n = 35$), differing between the upper and lower reaches,

Table 3

Summary of trace element concentrations of topsoil samples in the Xijiang River ($\mu g \cdot g^{-1}$).

Subjects	Ba	Li	Sr	Mn	P	Cd	Zn	Cu	Pb	As	Ni	Sb	Cr	pH	Zn/Cd
The Xun River upstream															
MIN	244.70	13.00	29.01	44.00	580.24	0.06	27.86	6.69	17.80	6.59	12.29	1.28	50.40	4.38	94.0
MAX	1053.00	60.47	71.00	3336.00	1250.62	1.56	146.53	46.58	123.91	22.32	38.54	8.62	106.20	7.78	500.9
MEAN	429.42	32.19	52.18	509.85	855.76	0.69	102.71	34.12	37.93	13.79	27.73	3.54	86.95	6.24	196.8
SD	189.64	9.01	10.13	566.74	153.75	0.43	28.92	7.80	18.80	4.70	6.37	2.01	12.70	0.69	97.4
The Xun River downstream															
MIN	428.84	19.71	18.04	101.10	402.44	0.14	47.79	25.26	36.35	7.06	20.74	1.20	72.60	4.79	101.5
MAX	625.40	45.07	83.90	759.20	1152.80	1.65	176.31	49.68	81.75	39.94	42.65	10.68	101.60	7.11	343.7
MEAN	497.43	31.02	47.76	446.54	769.87	0.94	117.03	37.13	48.54	20.38	30.57	5.08	85.87	5.85	147.4
SD	56.63	7.05	15.56	186.09	210.56	0.44	35.92	7.24	10.53	8.07	6.31	2.74	7.84	0.67	62.0
The Meng River															
MIN	231.70	12.78	12.62	93.36	479.30	0.08	35.68	14.07	20.00	5.77	9.71	0.89	42.20	4.56	141.5
MAX	665.87	32.58	63.53	538.38	1223.80	0.68	184.20	133.13	794.76	282.99	26.99	13.17	92.70	6.08	636.9
MEAN	437.78	19.19	26.31	185.91	814.97	0.23	68.13	29.23	80.58	39.05	19.87	2.26	73.58	4.97	334.8
SD	97.20	4.53	12.39	84.18	160.10	0.14	28.78	20.72	127.92	53.91	4.12	2.67	10.49	0.29	88.7
Chentang tributary of the Meng River															
MIN	403.73	14.33	16.76	102.10	652.00	0.12	39.90	19.17	23.77	7.21	16.99	0.58	69.10	4.92	233.5
MAX	462.14	18.59	33.98	217.30	1140.00	0.26	59.55	25.04	42.05	15.09	20.28	1.00	79.30	5.13	390.1
MEAN	436.34	16.72	26.41	158.55	838.34	0.16	48.10	22.41	29.08	10.78	18.78	0.83	74.50	5.05	309.1
SD	22.88	1.75	7.25	44.36	194.72	0.05	7.38	2.31	7.47	3.10	1.25	0.18	4.47	0.08	64.0
The Beiliu River															
MIN	186.70	21.99	21.98	81.56	339.00	0.08	31.96	8.72	20.71	2.95	7.61	0.35	27.40	4.89	104.2
MAX	456.30	80.81	117.60	531.80	914.00	1.22	126.65	37.46	48.34	19.72	32.88	6.28	79.30	6.41	701.8
MEAN	268.77	38.12	49.11	200.42	564.19	0.20	61.31	16.81	34.95	7.70	15.68	1.43	49.56	5.20	383.9
SD	62.72	14.49	20.31	100.27	157.08	0.20	18.77	6.18	8.75	4.34	5.38	1.20	13.48	0.30	114.2

Table 4

Summary of trace element concentrations of stream sediments in the Xijiang River ($\mu g \cdot g^{-1}$).

Subjects	Ba	Li	Sr	Mn	P	Cd	Zn	Cu	Pb	As	Ni	Sb	Cr	Zn/Cd
The Xun River upstream														
MIN	400.0	18.6	52.4	769.0	420.0	0.64	87.00	23.30	31.10	15.90	19.40	2.99	39.00	67.5
MAX	850.0	37.3	87.4	2050.0	859.2	4.22	285.00	58.90	131.16	50.00	40.20	8.48	85.90	149.4
MEAN	598.2	30.6	68.9	1269.7	667.5	1.56	164.36	38.96	60.37	27.93	31.72	5.72	63.39	111.1
SD	134.9	5.3	9.2	293.8	115.6	0.70	42.32	8.32	26.52	6.29	4.78	1.25	10.48	17.4
The Xun River downstream														
MIN	394.5	24.1	51.9	997.8	651.0	0.98	126.65	31.46	35.76	23.84	28.00	4.40	59.20	84.1
MAX	737.0	45.1	82.8	1856.4	1199.0	2.39	423.47	61.06	89.20	56.04	46.15	9.97	134.10	182.0
MEAN	571.8	36.5	69.4	1354.0	908.1	1.64	210.17	46.05	63.03	38.28	37.97	7.67	94.33	130.0
SD	89.7	5.1	9.4	282.2	177.2	0.43	73.24	8.67	15.34	11.74	4.87	1.60	23.21	28.0
The Meng River														
MIN	170.0	6.9	10.8	151.0	170.0	0.37	49.00	10.80	25.30	17.00	8.60	1.00	24.00	109.6
MAX	5240.0	40.6	139.5	3820.0	1400.0	20.80	2870.00	229.00	1215.00	2030.00	56.20	20.80	115.00	258.7
MEAN	1428.9	24.9	40.0	1001.8	724.8	7.37	1008.30	60.31	183.29	166.93	33.49	5.20	75.59	145.8
SD	1311.0	9.0	26.4	810.6	313.6	6.12	832.82	44.05	264.71	411.18	13.70	4.09	23.52	37.1
Chentang tributary of the Meng River														
MIN	190.0	8.0	13.9	185.0	180.0	0.24	85.00	8.90	12.90	8.20	11.10	0.91	25.00	137.1
MAX	750.0	32.0	39.0	1530.0	1440.0	13.85	2230.00	106.00	189.00	104.00	47.80	5.30	101.00	354.2
MEAN	500.0	19.9	25.9	686.0	612.5	5.21	839.50	40.45	84.33	44.76	29.44	2.87	60.75	189.9
SD	230.8	9.3	8.1	434.4	411.2	4.62	730.79	31.12	65.91	31.64	14.12	1.38	27.40	69.8
The Beiliu River														
MIN	310.0	23.2	44.7	296.0	370.0	0.12	73.00	15.90	35.40	17.20	17.40	1.37	40.00	261.5
MAX	490.0	55.7	62.5	1150.0	2370.0	0.55	218.00	51.60	148.00	82.30	38.50	11.75	195.00	1175.0
MEAN	423.0	39.1	52.5	765.0	1137.0	0.34	133.60	36.08	86.78	36.58	25.05	5.06	81.00	498.5
SD	54.8	10.4	6.0	320.6	592.3	0.17	43.10	11.59	34.23	19.35	6.48	3.07	51.43	300.4

which have ranges of 0.15‰–0.29‰ and − 0.05‰–0.1‰, respectively.

Topsoil samples from near the Meng River have a narrow range of $\delta^{114/110}$Cd values (−0.34‰ to 0.12‰; mean − 0.24‰ ± 0.06‰; 1SD, n = 14), with a wider range in stream sediments (−0.27‰ to 0.31‰; mean − 0.14‰ ± 0.14‰; 1SD, n = 27; Table 6).
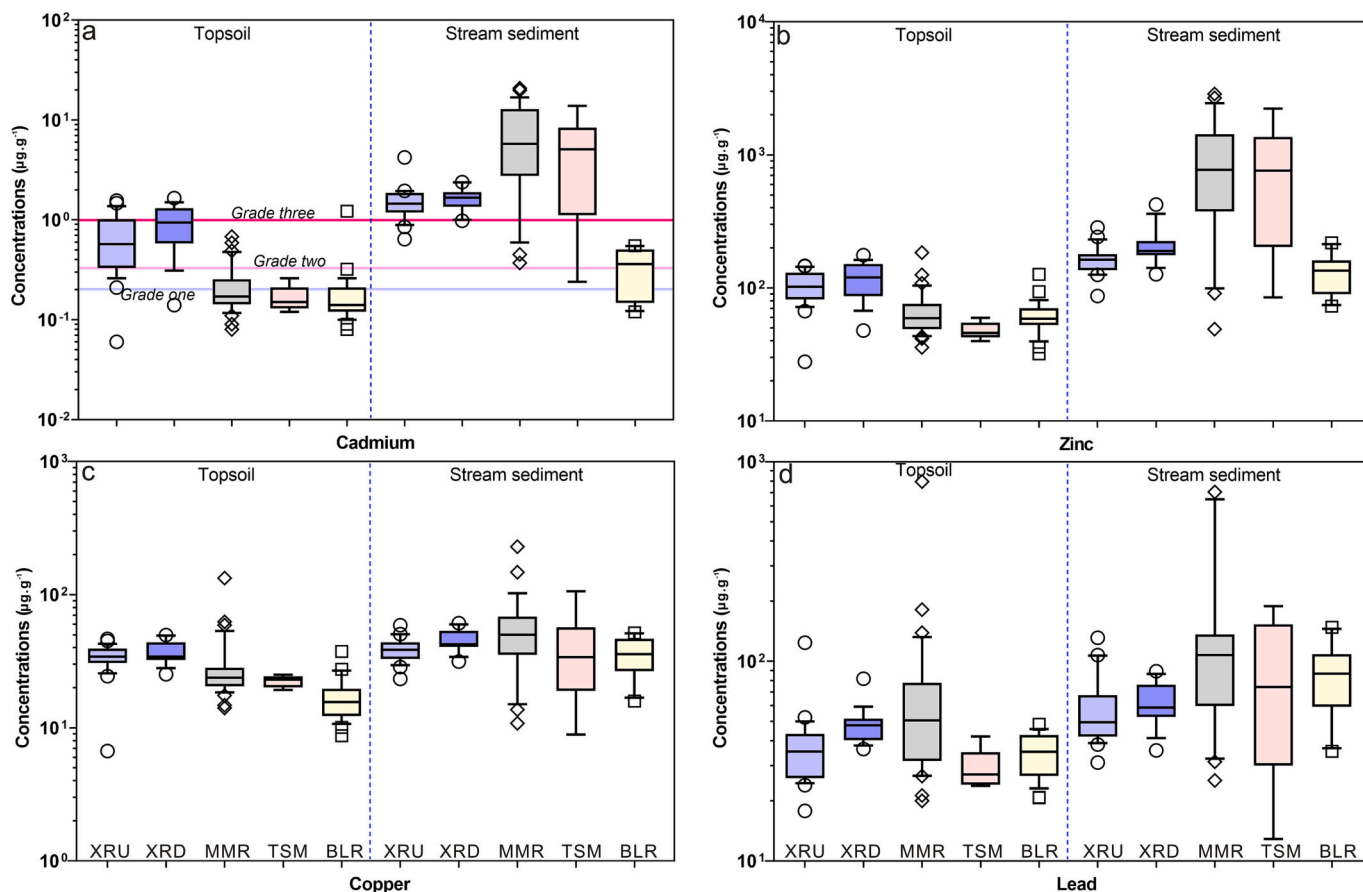
Fig. 2. Boxplots of heavy metals (Cd, Zn, Cu, and Pb) concentrations of topsoil and stream sediments in the Xijiang River.
(XRU: the Xun River upstream; XRD: the Xun River downstream; MMR:Meng River; TSM: Chengtang section of the Meng River; BLR: Beiliu River)

4. Discussion

4.1. Heavy-metal distributions

Topsoils from near the Xun River tend to have elevated Cd and Zn contents, whereas Pb and As contents are at natural background levels (Figs. 2 and S2). Cadmium contents are above Chinese national second-grade standards for soil (1.0 µg.g^{-1}; Environmental Quality Standards of China, GB15618-1995). The sediments are relatively enriched in heavy metals with average Cd, Zn, Pb, and As contents being 2.0, 1.7, 1.4, and 1.9 times those of average topsoil levels, respectively.

In lower river reaches, topsoil Cd contents fluctuate little, whereas sediment Cd contents increase slightly below the confluence of the Xun and Meng rivers. Indeed, most stream sediment heavy-metal contents are higher below the confluence, particularly for Zn (Figs. 2, 3a–b and S2). The Meng River is thus more seriously polluted than the Xun River, and it transports heavy metals downstream.

Topsoils near the Meng River have lower Cd and Zn contents than those near the Xun River, with relatively minor variations in the profile in lower river reaches, although their Pb and As contents are higher (Fig. 2). The Cd content averages 0.23 µg.g^{-1}, near the Chinese national first-grade standard for soil (0.20 µg.g^{-1}; GB15618-1995). However, stream sediment samples are enriched in Cd and other heavy metals (Fig. 2), with average Cd, Zn, Pb, and As contents 32.0, 14.7, 2.3, and 4.3 times those of topsoils, respectively. The Cd and Zn contents are also characterized by extreme variability through the downstream profile. The enrichment of sediments in both Cd and Zn indicates that the Meng River carries exogenous pollution (Song et al., 2018; Ren et al., 2017; Li et al., 2022).

Compared with the Xun and Meng rivers, the Beiliu River is relatively free of pollution (Figs. 2 and S2), and the Cd contents of topsoil and stream sediment samples are near background values for the region.

4.2. Lithological control of Cd in the Xun River

Above its confluence with the Meng River, the δ$^{114/110}$Cd values of topsoil and stream sediment samples for the Xun River are relatively uniform, ranging from −0.41‰ to −0.21‰ and from 0.17‰ to 0.29‰, respectively (Fig. 4a). Cadmium isotopic fractionation between stream sediments and topsoils is stable in the range of Δ$^{114/110}$Cd$_{stream\ sediment–topsoil}$ = 0.44‰–0.61‰ (average 0.50‰ ± 0.04‰; 1SD, n = 21). Below the confluence, the δ$^{114/110}$Cd values of topsoils are consistent with those of the upper river reaches at −0.35‰ to −0.12‰, whereas the values for stream sediment samples are lower at −0.05‰ to 0.15‰. Δ$^{114/110}$Cd$_{sediment–topsoil}$ values decrease significantly to a minimum of 0.17‰. Further downstream, the Cd isotopic fractionation between stream sediments and topsoils gradually returns to values recorded in the upper reaches of the Xun River (Fig. 4a).

Synthetic carbonate experiments have shown that calcite precipitated from fresh water shows no Cd isotopic fractionation between solution and calcite (Horner et al., 2011); fractionation is minor during calcite deposition from low-ionic-strength fluids (Wasylenki et al., 2014) and negligible, with high HCO$_3^-$ contents in such water (Xie et al., 2021). The pH values of topsoil samples collected from the upper reaches of the Xun River range from 4.38 to 7.78 (average 6.24 ± 0.69; 1SD, n = 29; Appendix A; Fig. 7). Conversely, the pH values of carbonate watershed of Xijiang River range from 7.38 to 8.19 (Wang et al., 2012; Zhai, 2020), which are similar with values from other carbonate watershed (Yaciuk et al., 2022). Bedrock in the upper Xun River region is dominated by Middle–Upper Devonian carbonate sediments (Pang, 2020) (Fig. 1).

Table 5

Cd isotopic composition of topsoil and stream sediment samples in the Xun River.

Topsoil				Stream sediment				$\Delta^{114/110}$Cd (‰)
Sample No.	Sampling distance (km)	$\delta^{114/110}$Cd (‰)	1σ	Sample No.	Sampling distance (km)	$\delta^{114/110}$Cd (‰)	1σ	
PN083	0.0	−0.23	0.03	PN-1	0.0	0.29	0.03	0.52
PN086	4.0	−0.26	0.05	PN-2	2.3	0.2	0.02	0.46
PN101	9.4	−0.21	0.04	PN-3	3.9	0.18	0.02	0.44
PN103	12.3	−0.31	0.02	PN-4	4.5	0.25	0.02	0.51
PN118	15.1	−0.41	0.05	PN-5	7.2	0.21	0.03	0.45
ML011	16.9	−0.35	0.04	PN-6	9.3	0.23	0.01	0.44
DA016	24.0	−0.26	0.02	PN-7	10.5	0.26	0.02	0.52
DA048	33.2	−0.31	0.03	PN-8	15.0	0.25	0.02	0.61
DA038	43.3	−0.28	0.02	PN-9	17.5	0.18	0.04	0.53
DA056	49.1	−0.23	0.03	PN-10	18.5	0.19	0.02	0.50
TX016	55.8	−0.12	0.01	PN-11	20.4	0.22	0.03	0.53
TX033	62.0	−0.28	0.03	PN-12	24.2	0.26	0.02	0.52
TX064	67.2	−0.26	0.02	PN-13	26.0	0.17	0.02	0.46
TX107	72.4	−0.31	0.06	PN-14	26.0	0.24	0.02	0.53
TX096	78.1	−0.29	0.03	DA031B1	26.1	0.22	0.01	0.51
TX084	84.3	−0.35	0.02	DA047D1	30.6	0.26	0.02	0.55
TX072	88.7	−0.31	0.03	DA048C1	32.0	0.22	0.03	0.51
TX084	84.3	−0.35	0.02	DA036D1	38.0	0.23	0.02	0.53
TX072	88.7	−0.31	0.03	DA037C1	38.5	0.23	0.03	0.53
				DA037D1	39.6	0.25	0.02	0.55
				DA056A1	44.9	0.18	0.02	0.44
				DA043B1	52.7	0.15	0.02	0.33
				TX031B1	56.6	0.1	0.01	0.30
				TX032A1	58.1	0.08	0.02	0.28
				TX033C1	60.4	−0.03	0.03	0.17
				TX048B1	61.9	−0.04	0.02	0.24
				TX049C1	63.4	−0.03	0.03	0.25
				TX063B1	65.4	−0.03	0.02	0.24
				TX063D1	66.2	−0.05	0.02	0.22
				TX064C1	67.1	0.01	0.02	0.27
				TX093C1	70.7	0.02	0.01	0.31
				TX108A1	72.1	0.02	0.02	0.33
				TX097B1	79.8	0.04	0.03	0.36
				TX083D1	82.5	0.04	0.02	0.36
				TX084B1	84.6	0.1	0.02	0.45

Table 6

Cd isotopic composition of topsoil and stream sediment samples in the Meng River.

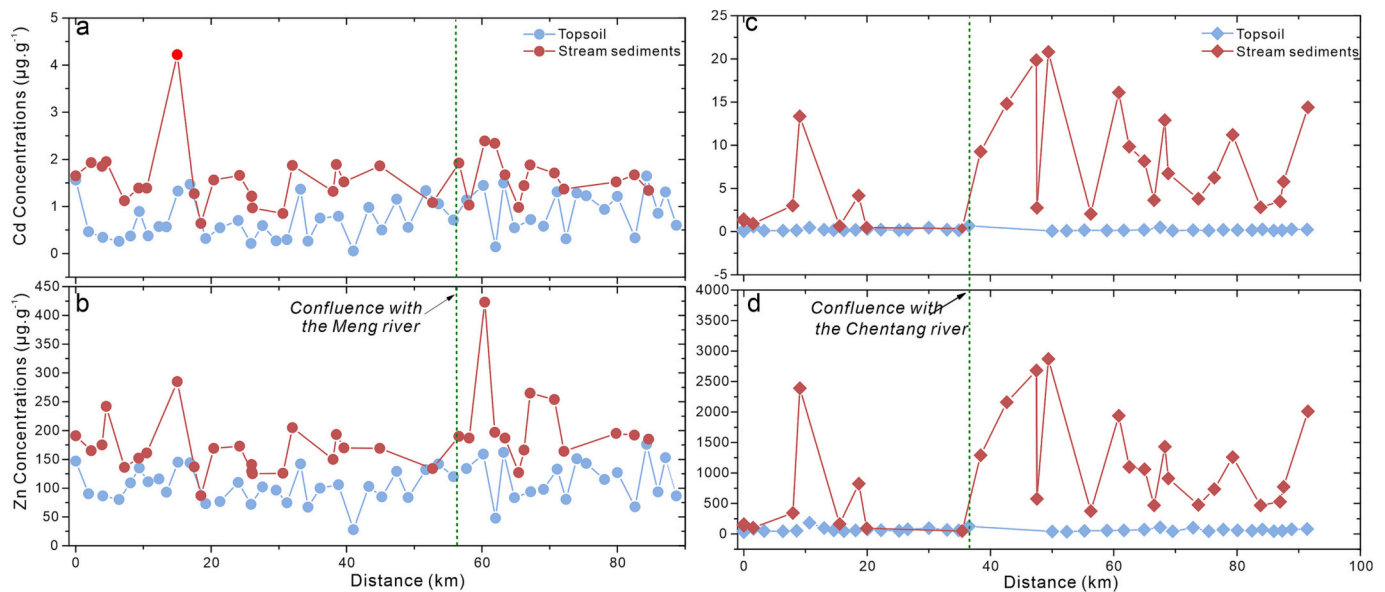| Topsoil				Stream sediment				$\Delta^{114/110}$Cd (‰)
Sample No.	Sampling distance (km)	$\delta^{114/110}$Cd (‰)	1σ	Sample No.	Sampling distance (km)	$\delta^{114/110}$Cd (‰)	1σ	
SY043	0.0	−0.21	0.03	DL-8	0.0	0.30	0.03	0.51
CT041	3.3	−0.23	0.05	DL-7	1.5	0.31	0.02	0.53
CT083	10.7	−0.2	0.04	DL-6	8.0	0.02	0.02	0.24
CT110	14.6	−0.31	0.02	DL-5	9.1	−0.15	0.03	0.05
CT124	18.1	−0.34	0.05	DL-4	15.5	−0.20	0.02	0.11
PT032	25.2	−0.21	0.02	DL-3	18.7	−0.20	0.03	0.14
PT049	33.0	−0.23	0.03	DL-2	19.9	−0.08	0.02	0.26
TZ010	50.0	−0.31	0.03	DL-1	35.4	−0.08	0.02	0.15
TZ039	58.9	−0.26	0.02	DR-2	38.4	−0.20	0.02	0.03
TZ052	64.9	−0.24	0.02	DR-1	42.7	−0.26	0.03	0.01
TZ097	72.9	−0.23	0.03	TP-6	47.5	−0.25	0.03	0.06
TZ113	80.1	−0.12	0.01	TP-5	47.6	−0.08	0.02	0.23
DA027	86.0	−0.31	0.03	TP-4	49.4	−0.20	0.04	0.11
DA014	91.4	−0.26	0.02	TP-3	56.3	−0.10	0.02	0.19
				TP-1	60.8	−0.23	0.02	0.02
				MJ-11	62.5	−0.27	0.01	−0.02
				MJ-10	65.0	−0.15	0.03	0.09
				MJ-9	66.6	−0.15	0.02	0.09
				MJ-8	68.3	−0.26	0.02	−0.02
				MJ-7-2	68.8	−0.16	0.03	0.08
				MJ-7	73.7	−0.18	0.02	0.05
				MJ-6	76.3	−0.15	0.02	0.03
				MJ-5	79.3	−0.26	0.04	−0.14
				MJ-4	83.8	−0.17	0.03	0.05
				MJ-3	87.0	−0.13	0.02	0.18
				MJ-2	87.5	−0.18	0.02	0.11
				MJ-1	91.5	−0.23	0.03	0.03

Fig. 3. Cd and Zn contents along downstream profile of the Xun River (a, b) and the Meng River (c, d).
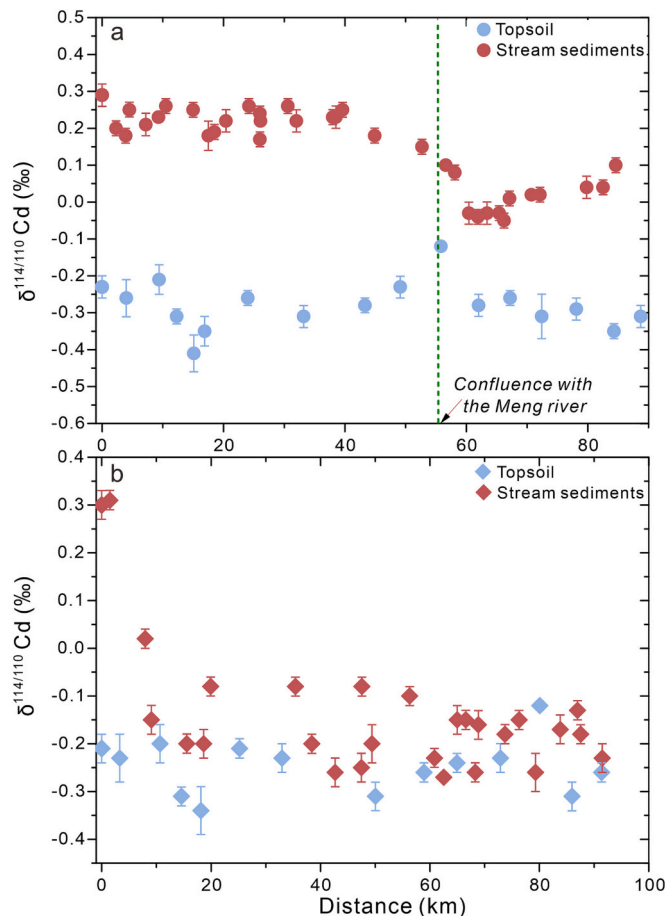

Fig. 4. Cd isotopic variations along downstream profile of the Xun River (a) and the Meng River (b).

Therefore, considering the long-term accumulation of sediments in the water column, stream sediments and their corresponding river water likely have analogous Cd isotopic compositions in the upper reaches of the Xun River. During chemical weathering, heavy Cd isotopes are preferentially enriched in the leachate during mineral dissolution and are absorbed on newly formed mineral phases (Zhang et al., 2016; Salmanzadeh et al., 2017; Zhu et al., 2018; Liao et al., 2022). Leaching experiments simulating the weathering processes indicate that heavy Cd isotopes are enriched in the leachate relative to initial and residual samples, with isotopic fractionation between leachate and residual states being $\Delta^{114/110}Cd_{leachate-residual} = 0.36‰–0.53‰$ (Zhang et al., 2016), similar to that between sediments and topsoil in the upper reaches of the Xun River. Comparable fractionation has been observed during sulfide mineral weathering in the Fule Zn—Pb deposit (Zhu et al., 2018). $\Delta^{114/110}Cd_{stream sediment-topsoil}$ values in the upper reaches of the Xun River thus indicate that Cd isotopic fractionation in sediments and topsoils is controlled mainly by natural weathering processes. It follows that the higher Cd contents recorded in the upper Xun River reaches are sourced mainly from the natural weathering of parent rocks.

Increasing alkalinity promotes Cd adsorption by Fe—Mn oxyhydroxides and its incorporation into other secondary minerals (Pan et al., 2014; Yan et al., 2021; Yaciuk et al., 2022; Fan et al., 2022), and increasing water-column pH leads to increased Cd adsorption on soils (Kuo and McNeal, 1984; Hao et al., 2001). Greenhouse experiments have shown that limestone mixed with Cd-contaminated soil increases soil pH and elevated the amounts of unexchangeable Cd in the soil (Yang et al., 2021). Under alkaline conditions, Cd^{2+} activity decreases by about two orders of magnitude through the formation of $CdCO_3$ nanoparticles (Street et al., 1978; Pan et al., 2014; Zhu et al., 2018; Li et al., 2021; Fan et al., 2022), which are virtually insoluble under such conditions. Such behaviour is consistent with the positive correlation between pH and Cd content in the topsoil and sediment samples (Fig. 5c, d). Cadmium and CaO geochemical anomalies are highly coincident in this region (Yang, 2009). Furthermore, the Zn/Cd ratios of sediments become increasingly similar to ratios in carbonate sediments with increasing Cd content (Fig. 5a; Zhu, 2013). This is more obvious for the sample of PN-08, which has the highest Cd contents but with normal $\delta^{114/110}Cd$ values in the stream sediments of the Xun River upstream. Zn/Cd ratio of PN-08 is 67.5 and falls into carbonate rocks range (Fig. 5a). Correspondingly, through the Xun River upstream, carbonate outcrops are the most common near the sample site of PN-08 (Fig. 1c). These observations suggest that an alkaline environment formed by carbonate weathering is a critical factor in Cd enrichment in the upper reaches of the Xun River, with the carbonate-dominated bedrock there playing an important role. Riverbank topsoils are relatively enriched in Cd, and a high-Cd belt following the Xun River is evident in the
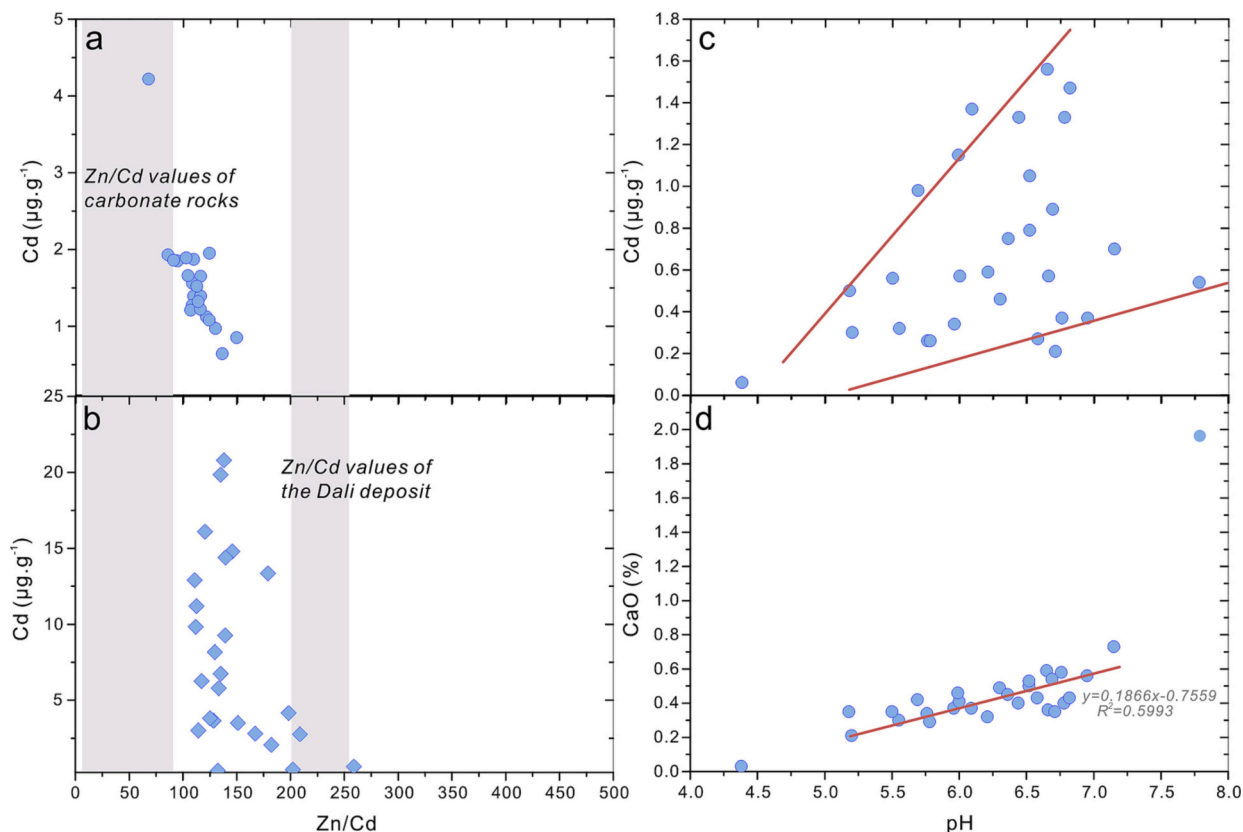
Fig. 5. Zn/Cd ratios for stream sediments samples of the Xun River (a) and the Meng River (b), pH values versus Cd contents (c) and CaO contents (d) plots of topsoil samples in the Xun River.
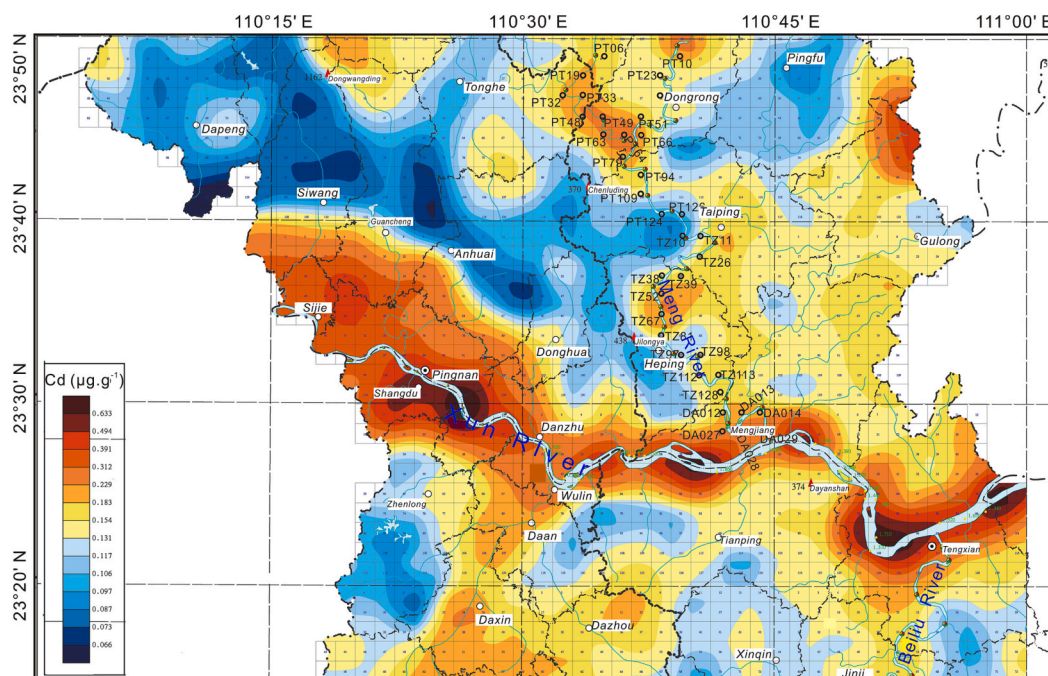

Fig. 6. Geochemical map of Cd in topsoil of the Xijiang River.

geochemical map (Fig. 6). We conclude, therefore, that during the weathering of carbonate sediments and soils in the upper reaches of the Xun River, Cd^{2+}, Ca^{2+}, and HCO_3^- in parent rocks are leached into the river, forming a weakly alkaline environment within the water column.

Long-term weathering results in the continued accumulation of Cd, ultimately forming high-Cd anomalies in stream sediments (Fig. S1). Cadmium accumulation is thus more likely in areas with carbonate sediments.

4.3. Effects of acid mine drainage on the Meng River

The Cd contents of the topsoil and stream sediment samples are near background levels in the headwaters of the Meng River, with average $\Delta^{114/110}Cd_{stream\ sediment-topsoil}$ values of 0.51‰ and 0.53‰, respectively (Fig. 4b), consistent with fractionation resulting from natural weathering. The Cd there is thus likely derived from natural sources. Downstream from the town of Dali, the Cd contents of stream sediments increase rapidly whereas those of topsoils do not change significantly (Fig. 3c–d). $\Delta^{114/110}Cd_{stream\ sediment-topsoil}$ values decrease downstream with a range of −0.14‰ to 0.26‰ (Fig. 4b). This Cd isotopic fractionation pattern is different to that indicated for natural weathering, suggesting that the higher Cd contents of sediments may be caused by anthropogenic activities.

The mountains surrounding the Meng River, especially near Dali, host large and economically significant Zn–Pb–Ag–(Au) deposits, with Cretaceous granitic magmatism having triggered the mineralization (Yang et al., 2017; Zhang et al., 2020) and the ore bodies having a close spatial connection with granitic intrusions. Under supergene conditions, mineralised veins, sulphides in stack ores, and mine wastes undergo oxidisation and/or decomposition reactions, leading to acid mine drainage and heavy-metal release (Rodriguez-Hernandez et al., 2021). During these reactions, S^{2-} is oxidised to S^{6+}, and Cd^{2+}, Zn^{2+}, and other metals in sphalerite are released into solution (Yaciuk et al., 2022). The Cd content of stockpiled sulphide ores decreases with increasing duration of erosion and leaching (Zhu et al., 2019). Mobilised Cd derived from tailing dams enters the river as a solid phase (Yang et al., 2019). Cadmium is markedly enriched in sphalerite, with Zn—Pb deposits thus usually having elevated Cd contents (Cook et al., 2009; Wen et al., 2016; Song et al., 2018; Yaciuk et al., 2022). The Pb, Zn, and Cd contents of ore samples collected from the Dali deposit average 10.0 wt%, 3.6 wt% and 168 µg.g^{-1}, respectively. Sphalerite in the Dali deposit contains ~2800 µg.g^{-1} Cd and is the main Cd carrier of the sulphides present. Large-scale mining of Pb and Zn ores has taken place in the area since 2002. Historical illegal mining operations have left mined ore and waste rock in randomly stockpiled ore dumps in the Dali area and in the downstream valley (Li et al., 2022), and intense sphalerite dissolution is expected to occur there. The generated acid mine drainage liberates large amounts of H$^+$ and Cd^{2+} to the aqueous system (Rodriguez-Hernandez et al., 2021; Yaciuk et al., 2022). Over the long term, such drainage results in an acidic water column, which promotes Cd transport over long distances and its accumulation in sediments (Figs. 3c–d and S1), resulting in high Zn and Cd contents in the Meng River water column and enrichment of Zn and Cd in stream sediments; Cu, Pb, and As also tend to accumulate. Furthermore, the observed Zn–Cd–Cu–Pb–As assemblage is consistent with that of the main mineralization of the Dali deposit (Fig. 2). The Zn/Cd ratios in polluted sediment samples range from 110.8 to 258.7. Although these ratios in water-based sediments differ from those of Pb—Zn ores, the ratios in sediments collected from the Meng River as it flows through the mining area are similar to those of Pb—Zn ores (Table 2). Sediment samples collected downstream of the mining area show an abrupt increase in Ba contents, to 1030–5240 µg. g^{-1} (average 2714 ± 1161 µg.g^{-1}; 1SD, $n = 11$; Fig. S1), representing 5–10-fold increases over upstream sediments. Downstream, the Meng River runs through the early Cambrian Huangdongkou Formation, which hosts many vein-type baryte deposits (Zhang, 1998). These deposits and related mining activities are the likely source of the relatively high Ba contents in the Meng River.

Cadmium content is positively correlated with Al$_2$O$_3$ content in polluted Meng River sediments (Fig. 7a, b), indicating that Cd may be adsorbed mainly on Al-bearing minerals in sediments, such as Al (hydro) oxides and aluminosilicates. Mineralogical analysis of suspended solids in the upper and lower regions of the Xijiang River Basin indicates that clay minerals are the major components of suspended solids in the silicate-rock region, with minor quartz, muscovite and goethite (Pang, 2020). The main types of clay mineral are kaolinite, chlorite, and illite (Pang, 2020). Clay minerals have strong adsorption and fixation abilities for heavy-metal ions, promoted by fine particles, large specific surface areas, and abundant variable charges (He et al., 2001; Sposito et al., 1999; Sherman, 2009; Hao et al., 2020). Acid mine drainage into the
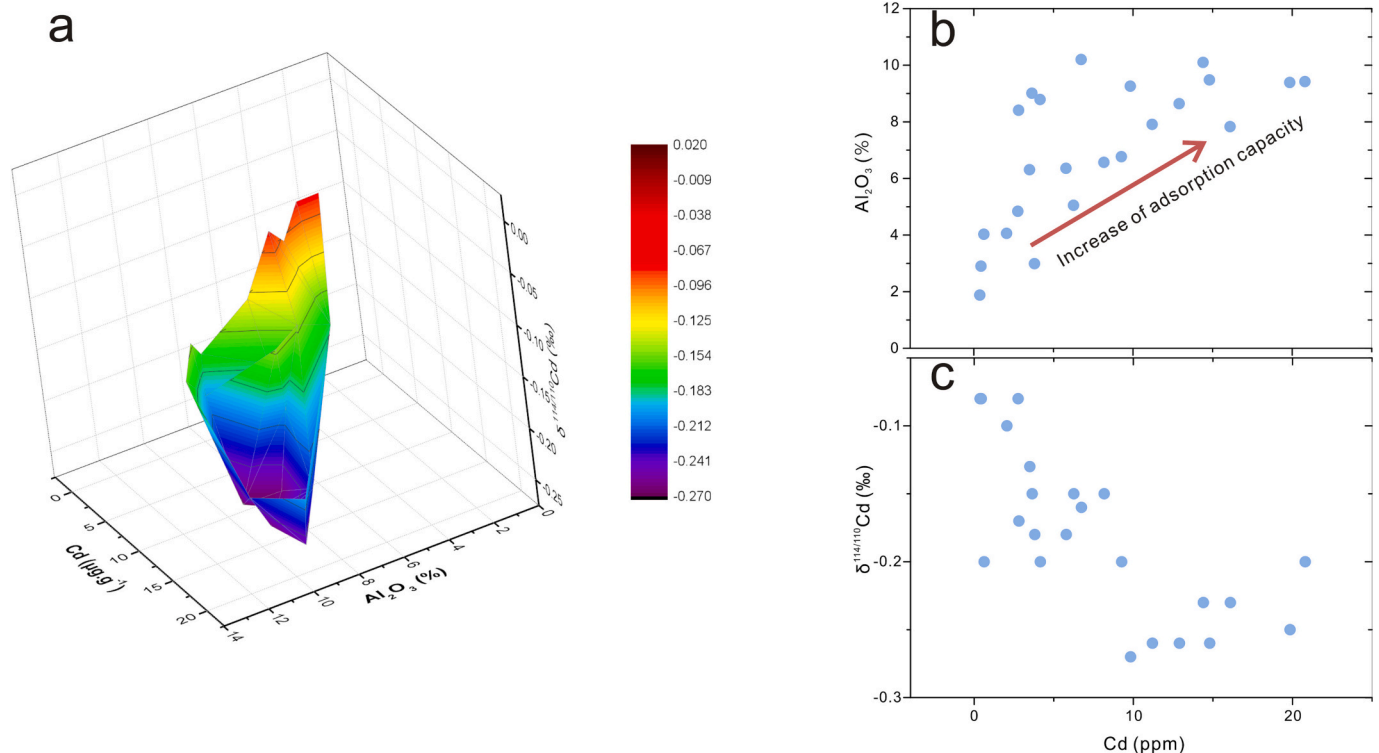

Fig. 7. (a) Plots of Cd concentrations, Al$_2$O$_3$ concentrations and δ$^{114/110}$Cd values of stream sediment samples in polluted Meng River; Cd concentrations versus Al$_2$O$_3$ concentrations (b) and δ$^{114/110}$Cd values (c) plots of stream sediments samples in polluted Meng River.

Meng River thus induces lower pH in the water column, and Cd^{2+} forms outer-sphere complexes on clay minerals under such conditions (Gräfe et al., 2007; Vasconcelos et al., 2008). Zinc isotopic fractionation between the solid phase and solution is minor through such complexation (Guinoiseau et al., 2017). $\Delta^{114/110}Cd_{solid-solution}$ values in the range of $-0.44‰$ to $-0.64‰$ are induced by adsorption on iron (oxyhydr)oxide surfaces (Yan et al., 2021), but such (oxyhydr)oxides occur only in trace amounts in suspended solids in the Meng River (Pang, 2020). The Cd isotopic composition of sediments is therefore likely to be similar to that of river water at low pH, where Cd is adsorbed by complexation with clay minerals. Furthermore, the Cd content has an inverse correlation with $\delta^{114/110}Cd$ values that of polluted sediments in the Meng River (Fig. 7c). The $\delta^{114/110}Cd$ value of the high-Cd stream sediments is about $-0.25‰$, and fall in the $\delta^{114/110}Cd$ ranges of the Jianzhupo deposit (Yang et al., 2023). During the deposition of stream sediments, the proportion of acid mine drainage water involved controls stream sediment Cd contents and isotopic variations.

A two-endmember model was developed to determine the relative contributions of acid mine drainage and unpolluted river water to the Cd isotopic compositions of sediments. Based on analytical results for the headwaters of the Meng River, C_1 and δ_1 are $1.14\ \mu g.g^{-1}$ and $0.305‰$, respectively, C_2 is $24.9\ \mu g.g^{-1}$ (Zhang et al., 2017), and the average $\delta^{114/110}Cd$ values of upper mineralization part of the Jianzhupo deposit are considered as δ_2 ($-0.35‰$; Yang et al., 2023). Based on a total annual flow of $3.8 \times 10^9\ m^3$ for the Meng River, V_1 and V_2 are in the range of $0-3.8$ (in $10^9\ m^3$). The $\delta^{114/110}Cd$ values of river water with different mixing ratios were calculated, and the two-endmember simulation indicates that (1) $\delta^{114/110}Cd$ values of the Meng River stream sediments are within the simulated range, (2) acid seepage from Pb—Zn ore is thus the main source of Cd in the Meng River, and (3) the major controller of Cd isotopic variations in stream sediment is acid mine drainage water, with minor amounts of acid mine drainage could being recorded in the Cd isotopic composition of stream sediments (Fig. 8b). The Cd isotope values of stream sediments of the Xun River upstream have a slight downward tendency before confluence with the Meng River (Fig. 4a). This probably results from the addition of minor amounts of acid seepage that contributed by some small tributaries around the Meng River (Fig. 1a).

A similar two-endmember model was developed to determine the relative contributions of waters of the Xun River water upstream and the Meng River water to Cd isotope of stream sediments of the Xun River downstream. C_1 and C_2 values were taken as the average Cd contents of stream sediments from the upper Xun and Meng rivers, respectively, where $C_1 = 4.56\ \mu g.g^{-1}$ and $C_2 = 8.07\ \mu g.g^{-1}$, and δ_1 and δ_2 are the average values for these sediments at $\delta_1 = 0.22‰$ and $\delta_2 = -0.18‰$. The Xun River has a total annual flow of $192.5 \times 10^9\ m^3$ with ranges of V_1 and V_2 being $0-192.5$ and $0-3.8$ (in $10^9\ m^3$) (Wang et al., 2012; Pang, 2020), respectively. The simulation indicated that lower sediment $\delta^{114/110}Cd$ values reflect higher proportions of Meng River water (Fig. 8a). This is consistent with the decrease observed in sediment samples from below the confluence of the two rivers. However, the annual flow of the Xun River is almost 50 times that of the Meng River, and stream sediment $\delta^{114/110}Cd$ values gradually return to their upstream values with an increasing proportion of Xun River water (Fig. 8a).

4.4. Cadmium source model

In the Xun river, the weathering of carbonate sediments and riverbank soils releases Cd^{2+}, Ca^{2+}, and HCO_3^- into the water column. The Cd isotopic composition of this leachate is controlled mainly by chemical weathering processes, $\Delta^{114/110}Cd_{leachate-topsoil}$ values average at $0.50‰$. Continued weathering results in the accumulation of Cd^{2+} and a weakly alkaline environment in the water column. Under these conditions, Cd^{2+} activity decreases rapidly with the formation of $CdCO_3$ nano-particles (Zhu et al., 2018; Fan et al., 2022), which are virtually insoluble under alkaline conditions and deposited in sediments (Fig. 9). $\Delta^{114/}$
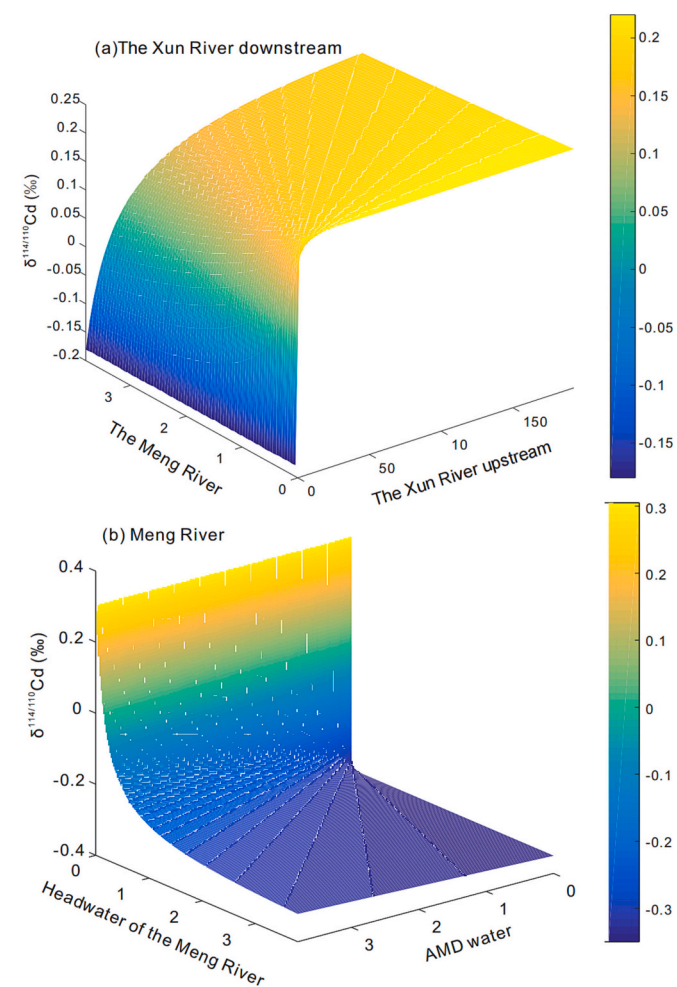

Fig. 8. Two-end-member simulation: (a) the contribution of the Xun river upstream water and the Meng river water to Cd isotope of stream sediments in the Xun river downstream, and (b) the contribution of the acid mine drainage water and unpolluted river water to Cd isotope of stream sediments in the Meng river. (the unit of runoff is 10^9 cubic meters).

$^{110}Cd_{sediment-topsoil}$ values are in the range of $0.44‰-0.61‰$, with an average of $0.50‰ \pm 0.04‰$ (1SD, $n = 21$).

In the Meng River, acid mine drainage from stockpiled ores and mine wastes liberates large amounts of H^+, Cd^{2+}, and other heavy metals into the aqueous system. Long-term drainage results in slightly acidic water-column environments, promoting Cd transport with accumulation of Cd in river water. There, Cd^{2+} forms outer-sphere complexes with clay minerals at low pH (Sherman, 2009), eventually being deposited with sediments (Fig. 9). $\Delta^{114/110}Cd_{stream\ sediment-topsoil}$ values become variable and are controlled mainly by the proportion of acid mine drainage in river water where sediment is deposited.

5. Conclusions and implications

During the chemical weathering of carbonate sediments and topsoils, Cd^{2+}, Ca^{2+}, and HCO_3^- in leachate cause the water-column to become alkaline, promoting the enrichment of Cd in stream sediments. Cd^{2+} activity decreases rapidly with the formation of $CdCO_3$ nano-particles and ultimately deposits in stream sediments. Cd isotopic fractionation between stream sediment and topsoil is stable, with an average $\Delta^{114/110}Cd_{stream\ sediment-topsoil}$ value of $0.50‰ \pm 0.04‰$.

In contrast, in sulphide-ore regions, acid mine drainage generated from stockpiled ores and mine wastes releases large amounts of H^+ and Cd^{2+} to the aqueous system. Long-term acid mine drainage results in
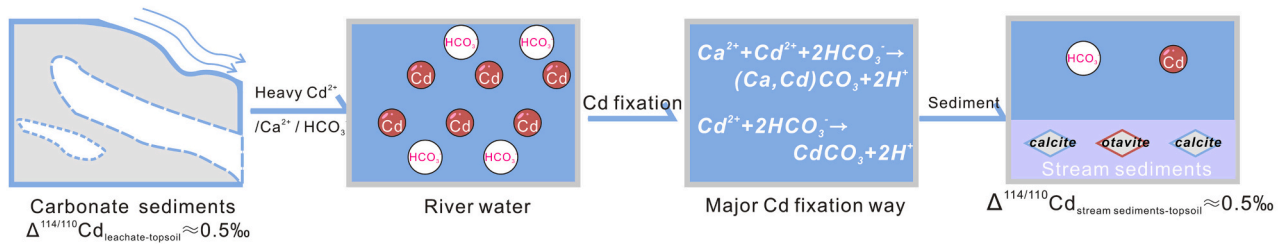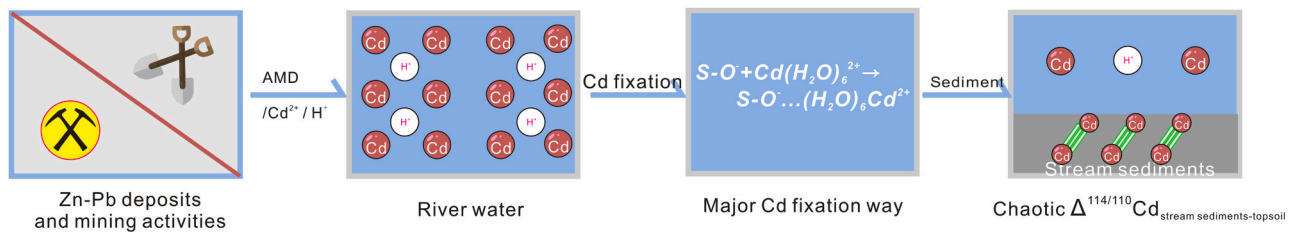
Fig. 9. Possible Cd source model in the Xijiang River. (a) Natural weathering of carbonate sediments promoted Cd^{2+}, Ca^{2+} and HCO_3^- drain into water columns by leachate. Cd^{2+} inclined to form $CdCO_3$ nano-particles under alkaline water columns and eventually deposited in the stream sediments. $\Delta^{114/110}Cd_{stream\ sediments-topsoil}$ is in the range of 0.44‰ to 0.61‰ (average in 0.50‰). (b) Acid mine drainage generated in piled ores and mine wastes liberate high amounts of H^+ and Cd^{2+} into the aqueous system. Cd^{2+} forms out-sphere complexes on the clay minerals under low pH environments. $\Delta^{114/110}Cd_{stream\ sediments-topsoil}$ in this situation was chaotic and mainly controlled by the proportion of acid mine drainage waters where stream sediments deposition.

slightly acidic environments in the water column, promoting Cd^{2+} transport and formation of outer-sphere complexes with clay minerals in stream sediments. In this situation, $\Delta^{114/110}Cd_{stream\ sediment–topsoil}$ values are variable and controlled mainly by the proportion of acid mine drainage water in the river.

Minor Cd isotopic fractionation in natural environments and industrial processes results in different geological repositories having generally overlapping ranges of Cd isotopic compositions, with limited scope for its application in clarifying Cd sources in complex systems. Nevertheless, $\Delta^{114/110}Cd_{stream\ sediment–topsoil}$ values could play a key role in distinguishing sources of Cd in a high ecological and/or an environmental health risk systems.

Declaration of Competing Interest

The authors declare that they have no known competing financial interests or personal relationships that could have appeared to influence the work reported in this paper.

Data availability

Data will be made available on request.

Acknowledgements

Appendix A. Supplementary data

Supplementary data to this article can be found online at https://doi.org/10.1016/j.chemgeo.2023.121571.

References

Aoshima, K., 2016. Itai-itai disease: renal tubular osteomalacia induced by environmental exposure to cadmium-historical review and perspectives. Soil Sci. Plant Nutr. 62, 319–326.

Cai, Y., 2015. A Study on Magmatism and Mineralization of the Damingshan Areas in the Central Guangxi Zhuang Autonomous Region, South China. Dissertation of Doctor Degree. Institute of Geochemistry, Chinese Academy of Sciences, Guiyang (in Chinese with English abstract).

CGS (China Geological Survey), 2005. Specification for Multi-Purpose Regional Geochemical Survey (DD2005-01). China Geological Survey, Beijing (In Chinese).

Chrastny, V., Cadkova, E., Vanek, A., Teper, L., Cabala, J., Komarek, M., 2015. Cadmium isotope fractionation within the soil profile complicates source identification in relation to Pb–Zn mining and smelting processes. Chem. Geol. 405, 1–9.

Cloquet, C., Carignan, U., Libourel, G., Sterckeman, T., Perdrix, E., 2006. Tracing source pollution in soils using cadmium and lead isotopes. Environ. Sci. Technol. 40, 2525–2530.

Cook, N.J., Ciobanu, C.L., Pring, A., Skinner, W., Shimizu, M., Danyushevsky, L., Saini-Eidukat, B., Melcher, F., 2009. Trace and minor elements in sphalerite: a LA-ICPMS study. Geochim. Cosmochim. Acta 73, 4761–4791.

Dai, S.F., Wang, P.P., Ward, C.R., et al., 2015. Elemental and mineralogical anomalies in the coal-hosted Ge ore deposit of Lincang, Yunnan, southwestern China: key role of N_2-CO_2-mixed hydrothermal solutions. Int. J. Coal Geol. 152 (A), 19–46.

Fan, T.T., Sun, Q., Cui, P.X., Xuan, L., Wang, Y.J., 2022. Sorption mechanism of cadmium on soils: a combination of batch experiment, path analysis, and EXAFS techniques. Geoderma 422, 115950.

Gao, B., Zhou, H.D., Liang, X.R., Tu, X.L., 2013. Cd isotopes as a potential source tracer of metal pollution in river sediments. Environ. Pollut. 181, 340–343.

Gräfe, M., Singh, B., Balasubramanian, M., 2007. Surface speciation of Cd(II) and Pb(II) on kaolinite by XAFS spectroscopy. J. Colloid Interface Sci. 315, 21–32.

Guinoiseau, D., Gelabert, A., Allard, T., Louvat, P., Moreira-Turcq, P., Benedetti, M.F., 2017. Zinc and copper behaviour at the soil-river interface: New insights by Zn and Cu isotopes in the organic-rich Rio Negro basin. Geochim. Cosmochim. Acta. 213, 178–197.

Hao, X.Y., Bao, D., Zhao, H., Guo, B.S., 2001. Absorption characteristic in the Yellow River. J. Inner Mongolia Normal Univ. (Nat. Sci. Edn.) 30 (2), 136–138 (in Chinese with English abstract).

Hao, W.D., Kashiwabara, T., Jin, R., et al., 2020. Clay minerals as a source of cadmium to estuaries. Sci. Rep. 10, 10417.

He, H.P., Guo, J.G., Zhu, J.X., Yang, D., 2001. An experimental study of adsorption capacity of montmorillonite–kaolinite and illite for heavy metals. Acta Petrol. Mineral. 20 (4), 573–578 (in Chinese with English abstract).

Horner, T.J., Rickaby, R.E.M., Henderson, G.M., 2011. Isotopic fractionation of cadmium into calcite. Earth Planet. Sci. Lett. 312, 243–253.

Kuo, S., McNeal, B.L., 1984. Effects of pH and phosphate on cadmium sorption by a hydrous ferric oxide. Soil Sci. Soc. Am. J. 48 (5), 1040–1044.

Li, C., Yang, Z., Yu, T., Hou, Q., Liu, X., Wang, J., Wu, T., 2021. Study on safe usage of agricultural land in karst and non-karst areas based on soil Cd and prediction of Cd in rice: a case study of Heng County, Guangxi. Ecotoxicol. Environ. Safety 208, 111505.

Li, C.X., Liu, Z.B., Gong, J.G., Wei, Z.Y., Zhang, Y.S., 2022. Heavy metal pollution characteristics of crops in downstream area of Dali lead-zinc mine in Tengxian County, Guangxi. Nonferrous Metals (Mining Section) 74 (1), 114–119 (in Chinese with English abstract).

Liao, R., Ratie, G., Shi, Z.M., et al., 2022. Cadmium isotope systematics for source apportionment in an urban–rural region. Appl. Geochem. 137, 105196.

Martinkova, E., Chrastny, V., Francova, M., Sipkova, A., Curik, J., Myska, O., Mizic, L., 2016. Cadmium isotope fractionation of materials derived from various industrial processes. J. Hazard. Mater. 302, 114–119.

MEPPRC (Ministry of Environmental Protection of the People''s Republic of China), MLRPRC (Ministry of Land and Resources of the People's Republic of China), 2014. Bulletin of National Survey of Soil Pollution. China.

Pallavicini, N., Engström, E., Baxter, D.C., Öhlander, B., Ingri, J., Rodushkin, I., 2014. Cadmium isotope ratio measurements in environmental matrices by MC-ICP-MS. J. Anal. At. Spectrom. 29 (9), 1570–1584.

Pan, Y., Koopmans, G.F., Bonten, L.T.C., Song, J., Luo, Y., Temminghoff, E.J.M., Comans, R.N.J., 2014. Influence of pH on the redox chemistry of metal (hydr)oxides and organic matter in paddy soils. J. Soils Sedim. 14 (10), 1713–1726.

Pang, S.Q., 2020. The Study on the Enrichment Mechanism of cd and Other Elements in the Xijiang River Basin. Master Degree Dissertation. China University of Geosciences, Beijing.

Ratie, G., Vankova, Z., Baragano, D., Liao, R., Sipkova, A., Gallego, J.R., Chrastny, V., Lewandowska, S., Ding, S., Komarek, M., 2022. Antagonistic Cd and Zn isotope behavior in the extracted soil fractions from industrial areas. J. Hazard. Mater. 439, 129519.

Ren, J., Liu, X.W., Wu, Y.X., Liu, X., Li, J., Wen, Z., 2017. Distribution characteristics of cadmium and arsenic in the tidal flat farmland soil and the river environment in the lower Xijiang River. Environ. Chem. 40 (7), 2168–2178 (in Chinese with English abstract).

Rodriguez-Hernandez, A., Lazaro, I., Razo, I., Briones-Gallardo, R., 2021. Geochemical and mineralogical characterization of stream sediments impacted by mine wastes containing arsenic, cadmium and lead in North-Central Mexico. J. Geochem. Explor. 221, 106707.

Salmanzadeh, M., Hartland, A., Stirling, C., Balks, M., et al., 2017. Isotope tracing of long-term cadmium fluxes in an agricultural soil. Environ. Sci. Technol. 51, 7369–7371.

Satarug, S., Ujjin, P., Vanavanitkun, Y., Nishijo, M., Baker, J.R., Moore, M.R., 2004. Effects of cigarette smoking and exposure to cadmium and lead on phenotypic variability of hepatic cyp2a6 and renal function biomarkers in men. Toxicology 204 (2–3), 161–173.

Scott, S.R., Smith, K.E., Dahman, C., Gorski, P.R., Adams, S.V., Shafer, M.M., 2019. Cd isotope fractionation during tobacco combustion produces isotopic variation outside the range measured in dietary sources. Sci. Total Environ. 688, 600–608.

Sherman, D.M., 2009. Surface complexation modelling: Mineral-fluid equilibria at the molecular scale. Rev. Mineral. Geochem. 70, 181–205.

Song, B., Yang, Z.J., Zhang, Y.X., Wang, F.P., Zhou, L., Zhong, X.M., 2018. Accumulation of Cd and its risks in the Soils of the Xijiang River Drainage Basin in Guangxi. Environ. Sci. 39 (4), 1888–1900 (in Chinese with English abstract).

Sposito, G., Skipper, N.T., Soper, A.K., 1999. Surface geochemistry of the clay minerals. Proc. Natl. Acad. Sci. U. S. A. 96 (7), 3358–3364.

Street, J.J., Sabey, B.R., Lindsay, W.L., 1978. Influence of pH, phosphorus, cadmium, sewage sludge, and incubation time on the solubility and plant uptake of cadmium. J. Environ. Qual. 7 (2), 286–290.

Vasconcelos, I.F., Haack, E.A., Maurice, P.A., Bunker, B.A., 2008. EXAFS analysis of cadmium(II) adsorption to kaolinite. Chem. Geol. 249, 237–249.

Wang, B., Lee, X.Q., Yuan, H.L., et al., 2012. Distinct patterns of chemical weathering in the drainage basins of the Huanghe and Xijiang River, China: evidence from chemical and Sr-isotopic compositions. J. Asian Earth Sci. 59, 219–230.

Wang, D.H., Xu, H., Zheng, Y.H., Gu, D.S., Xu, L.W., 2020. Environmental exposure to lead and cadmium and hearing loss in Chinese adults: a case-control study. PLoS One 15 (5), 0233165.

Wasylenki, L.E., Swihart, J.W., Romaniello, S.J., 2014. Cadmium isotope fractionation during adsorption to Mn oxyhydroxide at low and high ionic strength. Geochim. Cosmochim. Acta 140, 212–226.

Wei, R., Guo, Q., Wen, H., Liu, C., Yang, J., Peters, M., et al., 2016. Fractionation of stable cadmium isotopes in the cadmium tolerant ricinus communis and hyperaccumulator solanum nigrum. Sci. Rep. 6, 24309.

Wei, R.F., Guo, Q.J., Tian, L.Y., Kong, J., Bai, Y., Okoli, C.P., Wang, L.Y., 2019. Characteristics of cadmium accumulation and isotope fractionation in higher plants. Ecotoxicol. Environ. Saf. 174, 1–11.

Wen, H.J., Zhang, Y.X., Cloquet, C., Zhu, C.W., Fan, H.F., Luo, C.G., 2015. Tracing sources of pollution in soils from the Jinding Pb-Zn mining district in China using cadmium and lead isotopes. Appl. Geochem. 52, 147–154.

Wen, H.J., Zhu, C.W., Zhang, Y.X., Cloquet, C., Fan, H.F., Fu, S.H., 2016. Zn/Cd ratios and cadmium isotope evidence for the classification of lead-zinc deposits. Sci. Rep. 6, 25273.

Wen, Y., Li, W., Yang, Z., Zhang, Q., Ji, J., 2020. Enrichment and source identification of Cd and other heavy metals in soils with high geochemical background in the karst region, Southwestern China. Chemosphere 245, 125620.

Xie, X.J., Yan, L., Li, J.X., Guan, C., Chi, Z.Y., 2021. Cadmium isotope fractionation during Cd-calcite coprecipitation: Insight from batch experiment. Sci. Total Environ. 760, 143330.

Yaciuk, P.A., Colombo, F., Lecomte, K.L., Micco, G.D., Bohe, A.E., 2022. Cadmium sources, mobility, and natural attenuation in contrasting environments (carbonate-rich and carbonate-poor) in the Capillitas polymetallic mineral deposit, NW Argentina. Appl. Geochem. 136, 105152.

Yan, J., Fischel, M., Chen, H., Siebecker, M.G., Sparks, D.L., 2020. Cadmium speciation and release kinetics in a paddy soil as affected by soil amendments and flooding-draining cycle. Environ. Pollut. 268 (Part B), 115944.

Yan, X.R., Zhu, M.Q., Li, W., et al., 2021. Cadmium isotope fractionation during adsorption and substitution with iron (oxyhydr)oxides. Environ. Sci. Technol. 55 (17), 11601–11611.

Yang, T., 2009. Geochemical characteristics and prospecting potential in Guigang-Pingnan Pb-Zn ore zone, Guangxi. Miner. Resour. Geol. 23 (1), 65–69 (in Chinese with English abstract).

Yang, Q.J., Zhu, C.W., Wen, H.J.Zhang, Y.X., Fan, H.F., Song, W.R., Wu, Y.Z., Zhou, C., Luais, B., 2023. Cd isotopic constraints on the sources of Zn-Sb deposits: a case study of the Jianzhupo Zn-Sb deposit, Guangxi Province, China. Geol. Soc. Am. Bull. (accepted).

Yang, Q.J., Sun, M.X., Qin, Y., Zhang, Q.W., 2017. Study on geochronology and geological significance of Dali granitoids of Dayaoshan, Guangxi. Miner. Resour. Geol. 31 (5), 843–853 (in Chinese with English abstract).

Yang, W.J., Ding, K.B., Zhang, P., et al., 2019. Cadmium stable isotope variation in a mountain area impacted by acid mine drainage. Sci. Total Environ. 646, 696–703.

Yang, Y., Li, Y.L., Wang, M.E., Chen, W.P., Dai, Y.T., 2021. Limestone dosage response of cadmium phytoavailability minimization in rice: a trade-off relationship between soil pH and amorphous manganese content. J. Hazard. Mater. 403, 123664.

Yin, X.Y., Wei, R.F., Chen, H.D., et al., 2021. Cadmium isotope constraints on heavy metal sources in a riverine system impacted by multiple anthropogenic activities. Sci. Total Environ. 750, 141233.

Zhang, Y.E., 1998. Ore characteristic and its geological significance of Qilingshan barite ore deposit at Guipin of Guangxi. Guangxi Geol. 11 (2), 25–28 (in Chinese with English abstract).

Zhang, Y., Wen, H., Zhu, C., Fan, H., Luo, C., Liu, J., Cloquet, C., 2016. Cd isotope fractionation during simulated and natural weathering. Environ. Pollut. 216, 9–17.

Zhang, F., Wang, S.L., Nan, Z.R., Ma, J.M., Li, Y.P., Zhang, Q., Chen, Y.Z., 2017. Immobilization of Cu, Zn, Cd and Pb in mine drainage stream sediment using Chinese loess. Chemosphere 181 (83), 91.

Zhang, Y., Wen, H., Zhu, C., Fan, H., Cloquet, C., 2018a. Cadmium isotopic evidence for the evolution of marine primary productivity and the biological extinction event during the Permian-Triassic crisis from the Meishan section, South China. Chem. Geol. 48, 110–118.

Zhang, J.L., Liu, P.F., Zhang, Q.W., Wen, M.L., Bai, L.A., 2020. Study of Dali Pb-Zn deposit genesis in Dayaoshan area, Guangxi: the redistribution of fluid inclusion and H-O-S isotopic data analysis. Miner. Resour. Geol. 34 (6), 1084–1093 (in Chinese with English abstract).

Zhai, S.Y., 2020. The behavior analysis and sourcing of heavy metals during weathering and pedogenesis in the upper reaches of the Pearl River. Dissertation of Master Degree of Nanjing University (in Chinese with English abstract).

Zhao, F.J., Ma, Y., Zhu, Y.G., Tang, Z., McGrath, S.P., 2015. Soil contamination in China: current status and mitigation strategies. Environ. Sci. Technol. 49 (2), 750–759.

Zhao, Y., Deng, Q., Lin, Q., Zeng, C., Zhong, C., 2020a. Cadmium source identification in soils and high-risk regions predicted by geographical detector method. Environ. Pollut. 263, 114338.

Zhong, Q.H., Zhou, Y.C., Tsang, D.C.W., Liu, J., Yang, X., Yin, M.L., Wu, S.J., Wang, J., Xiao, T.F., Zhang, Z.F., 2020. Cadmium isotopes as tracers in environmental studies: a review. Sci. Total Environ. 736, 139585.

Zhong, Q., Wu, H.B., Niu, Q.S., Jia, P.P., Huang, F., 2021. Exposure to multiple metals and the risk of hypertension in adults: a prospective cohort study in a local area on the Yangtze river, China. Environ. Int. 153 (1), 106538.

Zhou, Z.B., Wen, H.J., 2021. A magmatic-hydrothermal indium-bearing polymetallic vein mineralization belt in the western Jiangnan Orogen: evidence from zinc and cadmium isotopes of sphalerite. Ore Geol. Rev. 131, 103843.

Zhu, C.W., 2013. Geochemistry of cd and Ge, and their Isotope in Carbonate-Hosted Lead-Zinc Ore Deposits in the Boundary Area of Sichuan, Yunnan and Guizhou Provinces, China. Doctor thesis of University of Chinese Academy of Sciences, Guiyang.

Zhu, C.W., Wen, H.J., Zhang, Y.X., Fu, S.H., Fan, H.F., Cloquet, C., 2017. Cadmium isotope fractionation in the Fule Mississippi Valley-type deposit, Southwest China. Miner. Deposita 52 (5), 675–686.

Zhu, C.W., Wen, H.J., Zhang, Y.X., Yin, R.S., Cloquet, C., 2018. Cd isotope fractionation during sulfide mineral weathering in the Fule Zn-Pb-Cd deposit, Yunnan Province, Southwest China. Sci. Total Environ. 616-617, 64–72.

Zhu, X.C., Cao, L.X., Liang, Y., 2019. Spatial distribution and risk assessment of heavy metals inside and outside a typical lead-zinc mine in southeastern China. Environ. Sci. Pollut. Res. 26, 26265–26275.